Quantifying Bimolecular Recombination Losses in Organic Bulk Heterojunction Solar Cells

Koster, L. Jan Anton; Kemerink, Martijn; Wienk, Martijn M.; Maturova, Klara; Janssen, Rene A. J.

[Link to publication in University of Groningen/UMCG research database](#)

COMMUNICATION

Quantifying Bimolecular Recombination Losses in Organic Bulk Heterojunction Solar Cells

L. Jan Anton Koster,* Martijn Kemerink, Martijn M. Wienk, Klará Maturová, and René A. J. Janssen

The amount of energy that the Earth receives from the Sun is enormous and dwarfs all non-renewable resources.[1] Recent developments of solar cells prepared from blends of conjugated polymers and fullerene derivatives have lead to significant steps forward in device efficiency, with the current record at 7.4% efficiency.[2] To enable a further improvement of organic solar cell efficiency a clear and thorough understanding of the fundamental processes that occur in organic solar cells is a necessity. One of the processes limiting the efficiency of organic solar cells is bimolecular recombination of photogenerated charge carriers[3–10] and in the quest for new high-performance materials it is important to establish just how many carriers are lost through this process.

We present a new and straightforward method to quantify what fraction of charge carriers recombine bimolecularly under operating conditions. This is achieved by accurately measuring the intensity dependence of the photocurrent. Our technique is much more precise than simply measuring the short-circuit current J_{sc} as a function of intensity I and easily resolves non-linear behavior that is obscured in conventional measurements. We find that bimolecular losses can amount to tens of percentages under solar illumination while J_{sc} versus I seemingly remains linear. This sheds new light on the importance of bimolecular recombination at short-circuit conditions. To analyze bimolecular recombination losses as a function of light intensity we derive a new analytical model for the photocurrent generated by a solar cell. It includes drift and diffusion of charge carriers as well as bimolecular recombination. By fitting this model to the experimental data of P3HT:PCBM cells, we find that the bimolecular recombination constant is suppressed relative to the Langevin rate.

The experimental technique developed to study the light intensity dependence of the photocurrent is based on measuring the differential current density ΔJ induced by a small modulation in

light intensity (ΔI) in the presence of a background light intensity I. This steady-state differential current (SSDC) measurement is carried out by illuminating the solar cell at short-circuit with a cw laser (wavelength 532 nm) and a mechanically modulated monochromatic light source of a much smaller intensity ΔI. A lock-in amplifier is used to pick up the current ΔJ induced by the modulated light source. By using a set of neutral density filters the intensity I of the cw light incident on the solar cell is modified. As a model system a blend of poly(3-hexylthiophene) (P3HT) and [6,6]-phenyl C_{61}-butyric acid methyl ester (PCBM) as electron donor and acceptor respectively, is used.

The current-voltage characteristics of these devices under simulated AM1.5G (1000 W m^{-2}) illumination are shown in **Figure 1**a. Figure 1b shows the steady-state differential current density ΔJ at short circuit as a function of intensity (average of laser and modulated light) for devices annealed at different temperatures. No stable signal could be obtained from the as-cast device, but the annealed devices did yield a stable steady state signal. Devices annealed at 100 °C or more give rise to differential current densities that show a plateau at low intensity. At these low intensities, the differential current does not depend on light intensity and, hence, we expect bimolecular losses to be negligible in this regime. The bimolecular recombination efficiency (η_{BR}) at higher light intensities can therefore be quantified by normalizing the data to the plateau value (ΔJ^{norm}) as $\eta_{BR} = 1 - \Delta J^{norm}$. At high intensities they amount to several percent, even for the most efficient devices. It should be noted that at approximately 300 W m^{-2} of the monochromatic light (532 nm) used here the resulting short-circuit current density is approximately equal to that obtained for standard solar light (AM1.5G) conditions. Hence, this light intensity is representative for normal operating conditions. At this light intensity, the losses amount to 2% for the device annealed at 130 °C, increasing to 17% for the device annealed at 100 °C. The loss in differential current obtained in this way represents the total of all intensity dependent losses. It does not, however, account for any losses that do not depend on intensity, such as geminate recombination, charge carrier diffusion, etc.

The device annealed at 70 °C displays a behavior that is quite different from the devices annealed at 100 °C or more. Firstly, no plateau is observed and, secondly, the dependence of ΔJ on light intensity appears to have a different functional form. It has been suggested that the intensity dependence of such devices is dominated by space-charge effects.[11] These factors render a full description of this device beyond the scope of the present work.

The data in Figure 1 imply that the current generated by P3HT:PCBM solar cells is not linearly proportional to incident light intensity. Several authors have used a power law to

Dr. L. J. A. Koster, Dr. M. Kemerink, Dr. M. M. Wienk, Dr. K. Maturová, Prof. R. A. J. Janssen
Molecular Materials and Nanosystems
Eindhoven University of Technology
PO BOX 513, 5600 MB Eindhoven, the Netherlands
E-mail: l.j.a.koster@rug.nl
Dr. L. J. A. Koster
Molecular Electronics
Zernike Institute for Advanced Materials
University of Groningen
Nijenborgh 4, 9747 AG Groningen, the Netherlands
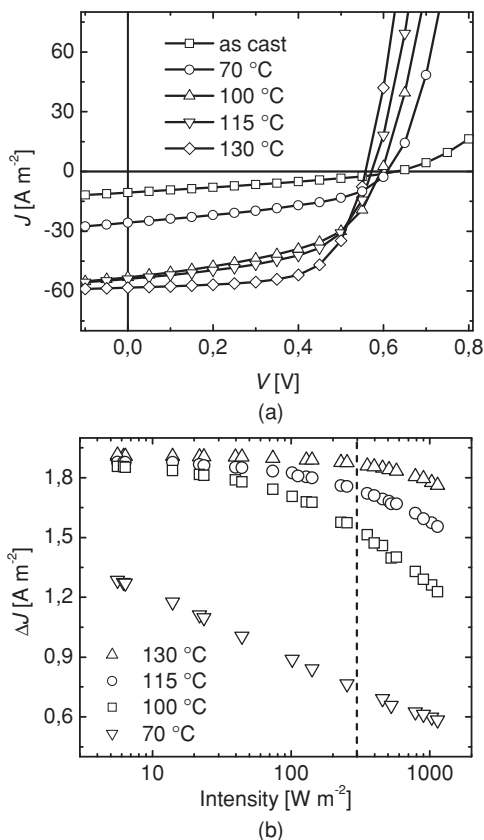E-mail: l.j.a.koster@rug.nl

Figure 1. (a) Current–voltage characteristics of a set of P3HT:PCBM devices annealed at different temperatures under simulated AM1.5G illumination. (b) The differential current density ΔJ as a function of intensity. The dashed line corresponds to light conditions that yield similar photocurrent as AM1.5G light.
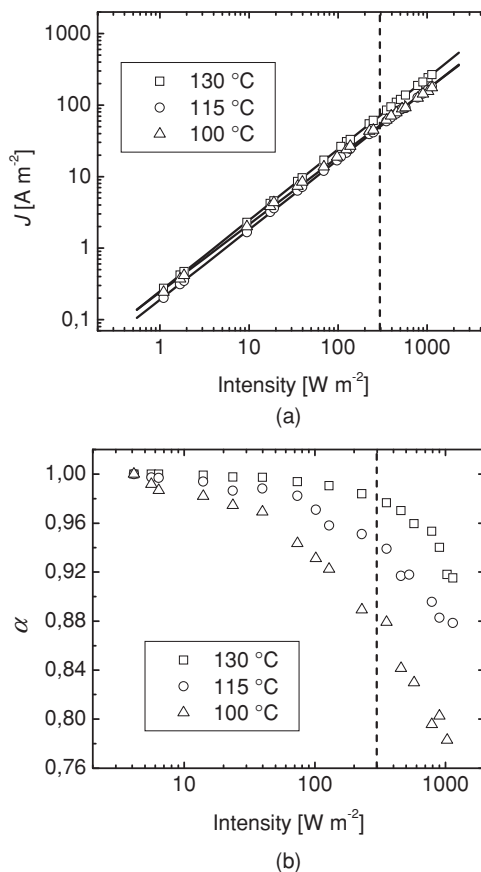

Figure 2. (a) The short-circuit current density of devices annealed at different temperatures as a function of light intensity at 532 nm (symbols) for P3HT:PCBM solar cells. Fitting a power law (line, Equation 1) to these data yields $\alpha = 0.945 \pm 0.006$ (100 °C), 0.980 ± 0.003 (115 °C), 0.994 ± 0.001 (130 °C). (b) The exponent α obtained by applying Equation 2. The dashed line corresponds to light conditions that yield similar photocurrent as AM1.5G light.

describe the dependence of the short-circuit current density J_{SC} on intensity I

$$J_{SC} \propto I^{\alpha}, \tag{1}$$

where α is close to unity, which is taken as indicative of weak bimolecular recombination.[12–19] In P3HT:PCBM solar cells, α strongly depends on annealing conditions and can deviate significantly from unity.[11] **Figure 2**a shows the short-circuit current versus intensity for the different devices. Fitting Equation 1 to these data yields $\alpha = 0.994$ for the device annealed at 130 °C down to $\alpha = 0.945$ for the device annealed at 100 °C. Clearly, in this procedure, differences between devices are only marginally visible. Moreover, a possible intensity dependence of α, as suggested by Figure 1b, is neglected.

To obtain α as a function of intensity, one can take the first derivative with respect to intensity and get α from $\alpha = (dJ/dI)(I/J)$. However, this requires knowing the ratio I/J (and preferably dJ/dI) to great accuracy. This is not easily achieved experimentally, leading to rather noisy values of α. Instead of obtaining α from Equation 1 by taking the first derivative, we take the second derivative with respect to I. As α is but a slowly varying function of I, terms containing its derivatives can be neglected and one has

$$\alpha = 1 + I \frac{d^2 J}{d I^2} \left(\frac{dJ}{dI} \right)^{-1}, \tag{2}$$

which yields α as a function of intensity. To obtain α from Equation 2, one can use the data plotted in Figure 1b and approximate $dJ/dI \approx \Delta J/\Delta I$. By differentiating these data once and applying Equation 2 we obtain α (see Figure 2b). Again we find that higher annealing temperatures lead to higher values of α. However, in contrast to Figure 2a, the SSDC method (Figure 2b) also yields the intensity dependence of α. Rather than being constant α decreases with increasing light intensity showing the importance of bimolecular recombination at moderate-to-high light intensities. The so-obtained values for α show little noise and small (<1%) deviations from unity are easily resolved.

An analytical model for the current-voltage characteristics of solar cells would be a great help when trying to interpret these experimental results. Here, we derive a simple closed analytical expression for the current density generated by a solar cell that includes drift and diffusion of charge carriers, as well as

bimolecular recombination. Consider a solar cell with charge carriers being photogenerated at a rate G and electrons (n) and holes (p) being extracted at rates f_n and f_p, respectively. The rate of change of the carrier densities is given by

$$\frac{dn}{dt} = G - f_n n - \gamma np, \tag{3}$$

for electrons and similarly for holes. Here γ is the bimolecular recombination constant. The extraction rates $f_{n,p}$ can be written as the sum of a term describing the drift of carriers and a term due to diffusion:

$$f_{n,p} = f_{n,p}^{\text{diffusion}} + f_{n,p}^{\text{drift}}. \tag{4}$$

The drift term is estimated as the inverse of the transit time,

$$f_{n,p}^{\text{drift}} = 2 \frac{\mu_{n,p} F}{L}, \tag{5}$$

where L is the active layer thickness and $\mu_{n,p}$ are the electron and hole mobility. Neglecting space-charge effects, the field strength F is taken as V/L, with V the effective voltage drop across the active layer. In Equation 5 L is divided by 2 since, on average, charges need to traverse only half of the active layer in order to reach an electrode. Similarly, the diffusion contribution is given by

$$f_{n,p}^{\text{diffusion}} = \frac{2 D_{n,p}}{(L/2)^2} = 8 \frac{\mu_{n,p} k_B T}{q L^2}, \tag{6}$$

where the Einstein relation has been used. In steady-state, the electron and hole rate equations are easily solved for the carrier densities;

$$p = \frac{f_p \mu_n}{2\gamma \mu_p} \left[\sqrt{1 + \frac{4\gamma \mu_p G}{f_p^2 \mu_n}} - 1 \right] \tag{7}$$

and $n = (\mu_p/\mu_n)p$.

As diffusion of carriers out of the device is bi-directional it does not contribute to the current density J in the external circuit. Hence, the only contribution to J stems from drift and one has $J = q f_p^{\text{drift}} pL$. In this framework, we can define the bimolecular recombination loss efficiency η_{BR} as the fraction of carriers lost due to bimolecular recombination, viz.

$$\eta_{BR} = \frac{\gamma np}{G} = \frac{\gamma p^2 \mu_p}{G \mu_n}, \tag{8}$$

where p is given by Equation 7. By assuming that the generation rate of free carriers G is proportional to light intensity and using Equation 1 we have

$$\eta_{BR} = \alpha^{-1} - 1. \tag{9}$$

Equations 8 and 9 provide a full description of the intensity dependence of the photocurrent generated by an organic solar cell. The current approach goes well beyond simple models that predict a linear dependence ($\alpha = 1$) of photocurrent on intensity in the absence of bimolecular recombination and $\alpha = \frac{1}{2}$ in the high intensity regime.[20,21] Equation 9 correctly shows that $\alpha = \frac{1}{2}$ (1) corresponds to a 100% (0%) efficient bimolecular

recombination mechanism. So, provided bimolecular recombination is the major intensity dependent loss mechanism and space-charge effects are not operative, one can now directly relate α to the fraction of charge carriers that are lost due to bimolecular recombination.

At this point it is important to establish if and when the assumption of a uniform electric field is appropriate. Space-charge effects are predicted to lead to $\alpha = 0.75$.[22] To assess whether space-charge effects influence the intensity dependence for $\alpha > 0.75$ we have performed numerical simulations[23] and compared these with the analytical model. In the numerical simulations the Poisson equation and current continuity equations were solved self-consistently. Generation of free charge carriers was assumed to be constant throughout the active layer (geminate recombination effects are neglected). The main difference between both approaches is that the numerical simulations spatially resolve the electric field and carrier densities which makes it possible to account for space charge effects. Mobilities typical for P3HT:PCBM devices annealed at 100 °C and 130 °C were used as input parameters.[24] At high intensities the numerical model indeed predicts α close to 0.75 (see **Figure 3a**). As the analytical model does not account for space charge, it fails to predict this value of α correctly. Instead, it predicts that α tends to 0.5 in the high intensity limit. According
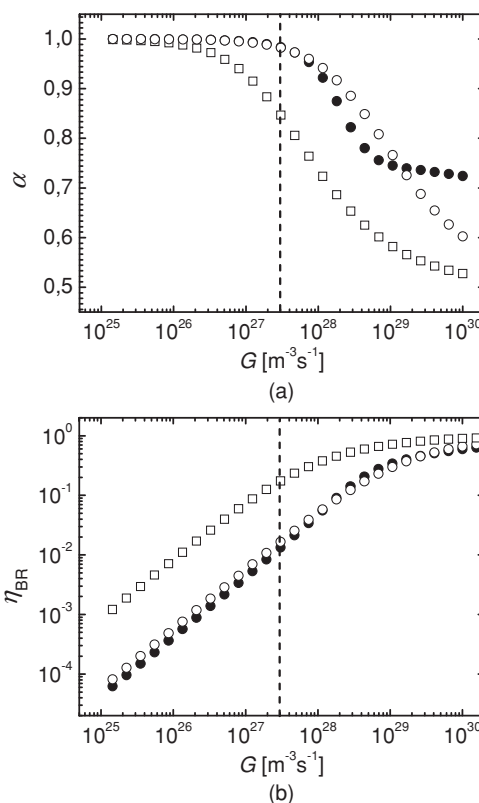

Figure 3. The (a) exponent α and (b) loss efficiency η_{BR} as obtained from numerical simulations (closed symbols) and the analytical model (open symbols) for P3HT:PCBM. Parameters are typical for P3HT:PCBM devices annealed at 100°C (squares) and 130°C (circles). The dashed line corresponds to conditions that would correspond to AM1.5G light.

to Equation 9 α = 0.5 corresponds to 100% efficient bimolecular recombination. In the numerical simulations this is not observed at the intensities studied here because, as space-charge effects become important, the internal electric field is adjusted such that hole extraction is facilitated. On the other hand, the agreement between numerical and analytical results is quite good for $\alpha > 0.75$. It is to be expected that this agreement holds for other material combinations as well. Figure 3b shows the predicted intensity dependence of the total loss efficiency η_{BR}. Again, the agreement between analytical and numerical results is quite good. These results imply that for $\alpha > 0.75$ the intensity dependence of the photocurrent is dominated by bimolecular recombination effects and that the analytical model can be used to analyze the experimental data in this regime.

The dependence of η_{BR} on light intensity obtained from $\eta_{BR} = 1 - \Delta J^{norm}$ is shown in **Figure 4**. As expected, these losses are highest for devices annealed at 100 °C and lowest for devices annealed at 130 °C. At low light intensities, η_{BR} is linearly proportional to light intensity for all devices: If η_{BR} is small the electron and hole densities are approximately linear in intensity and it follows from Equation 8 that η_{BR} should be linear in intensity if $\eta_{BR} \ll 1$. As the losses amount to approximately 10% or more, η_{BR} starts to level off. Equation 9 can also be used to calculate η_{BR}, see Figure 4. Good agreement between both methods is obtained, showing the validity of the current approach and Equation 9. The latter implies that the measured light intensity dependent losses are indeed related to bimolecular recombination.

Bimolecular recombination in organic bulk heterojunction solar cells has been found to be reduced with respect to the Langevin rate:[3–8] $\gamma = \gamma_{pre}(q/\varepsilon)(\mu_n+\mu_p)$, where $\gamma_{pre} \ll 1$. An estimate of the prefactor γ_{pre} can be obtained by fitting the data in Figure 4 to Equation 8. To this end, we take the values of the electron and hole mobilities from the literature[24] and relate the generation rate of free carriers G to light intensity I as $qGL = cI$, where c is a constant related to the optical properties of the

materials used. The voltage across the active layer is estimated to be 0.6 V, which is slightly larger than the observed open-circuit voltage of these devices. Rather good agreement between the data and the analytical model was found for recombination prefactors γ_{pre} ranging from 0.09 (130 °C) to 0.3 (100 and 115 °C), showing that bimolecular recombination is indeed reduced relative to the Langevin rate. Deibel et al.[6] have reported a similar trend.

In sum, we have presented a new, accurate and simple method for studying the intensity dependence of the photocurrent generated by organic solar cells. It enables the direct experimental determination of intensity dependent losses and can be generally applied to organic solar cells. Moreover, we derived an analytical model to quantitatively relate these losses to bimolecular recombination. This model offers a direct link between the bimolecular recombination loss efficiency (η_{BR}) and the intensity dependence of the short circuit current as $\eta_{BR} = \alpha^{-1} - 1$, where α is the exponent of the intensity (I) dependence of the short circuit current $J_{SC} \propto I^\alpha$. In the case of P3HT:PCBM these losses can amount to 17% for devices annealed at 100 °C under solar illumination. Additionally, the analytical model affords an estimate of the bimolecular recombination constant. We find for the P3HT:PCBM system that recombination is suppressed relative to the Langevin rate by a factor of three for devices annealed at 100 and 115 °C, and by one order of magnitude for devices annealed at 130 °C.

Experimental Section

Materials: The materials used were regio-regular poly(3-hexylthiophene) (P3HT) (Rieke Metals, molecular weight M_w = 66 kg mol^{-1}, polydispersity index 2.1) and poly(3,4-ethylenedioxythiophene):poly(styrene sulfonate) (PEDOT:PSS) from H.C. Starck Clevios GmbH (Clevios P VPAI 4083). PCBM was purchased from Solenne b.v.

Sample preparation: For photovoltaic device preparation, cleaned indium tin oxide (ITO) covered glass substrates, with an active area ranging from 0.1–1.0 cm^2, were covered with a 50 nm thick layer of PEDOT:PSS by spin casting in ambient conditions. The active layer, consisting of P3HT and PCBM (1:1 by weight), was spin cast from a chlorobenzene solution (15 mg mL^{-1}). A 1 nm thick layer of lithium fluoride (LiF) and a 100 nm thick aluminum layer were deposited by thermal evaporation under vacuum (<10^{-6} mbar). Current-voltage characteristics were recorded with a computer controlled Keithley 2400 source meter under a nitrogen atmosphere. Film thicknesses were measured with a Dektak 150 stylus profiler (Veeco). Simulated solar light (~1000 W m^{-2}) from a tungsten-halogen lamp filtered by a Schott GG385 UV filter and a Hoya LB120 daylight filter was used to illuminate the devices.

SSDC Measurements: A 532 nm cw laser is used to illuminate the solar cell under investigation. With a lens the beam is spread to ensure the device is illuminated by a uniform intensity profile. A set of 12 neutral density filters is used to modify the intensity of this beam. The white light of a 12 V halogen lamp is modulated with a mechanical chopper and passed through a monochromator set to 532 nm. A lock-in amplifier is used to measure the differential current density ΔJ by measuring the voltage across a 50 Ohm resistance. A calibrated silicon photodiode is used to measure the light intensity. During the measurements the sample was kept in a nitrogen filled sample holder. To verify that the measured ΔJ corresponds to steady-state conditions the modulation frequency is varied from 40 to 240 Hz. No change in signal was observed and the chopper was set to 170 Hz for the remainder of the experiments.
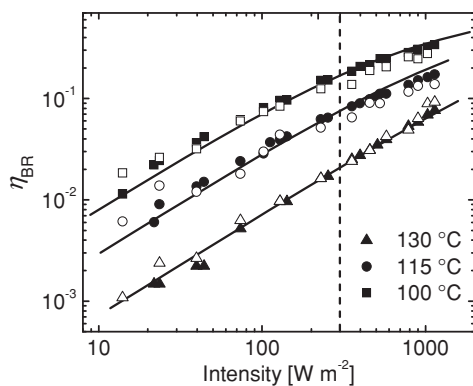

Figure 4. Loss efficiency $\eta_{BR} = 1 - \Delta J^{norm.}$ (closed symbols) for P3HT:PCBM devices annealed at different temperatures and fits to Equation 8 (lines) using electron and hole mobilities from [24]: $\mu_n = 1.9 \times 10^{-7}$ m^2·V^{-1}·s^{-1} and $\mu_p = 3.7 \times 10^{-9}$ m^2·V^{-1}·s^{-1}, $\mu_n = 2.8 \times 10^{-7}$ m^2·V^{-1}·s^{-1} and $\mu_p = 8.9 \times 10^{-9}$ m^2·V^{-1}·s^{-1}, and $\mu_n = 3.7 \times 10^{-7}$ m^2·V^{-1}·s^{-1} and $\mu_p = 1.5 \times 10^{-8}$ m^2·V^{-1}·s^{-1}, for devices annealed at 100, 115, and 130 °C, respectively. The open symbols refer to η_{BR} obtained by applying Equation 9 to the data in Figure 2b. The dashed line corresponds to light conditions that yield similar photocurrent as AM1.5G light.

Acknowledgements

[1] O. Morton, *Nature (London)* **2006**, *443*, 19.

[2] Y. Liang, Z. Xu, J. Xia, S.-T. Tsai, Y. Wu, G. Li, C. Ray, L. Yu, *Adv. Mater.* **2010**, *22*, E135.

[3] A. Pivrikas, G. Juška, A. J. Mozer, M. Scharber, K. Arlauskas, N. S. Sariciftci, H. Stubb, R. Österbacka, *Phys. Rev. Lett.* **2005**, *94*, 176806.

[4] G. Juška, G. Sliaužys, K. Genevicius, K. Arlauskas, A. Pivrikas, M. Scharber, G. Dennler, N. S. Sariciftci, R. Österbacka, *Phys. Rev. B* **2006**, *74*, 115314.

[5] C. G. Shuttle, B. O'Regan, A. M. Ballantyne, J. Nelson, D. D. C. Bradley, J. R. Durrant, *Phys. Rev. B* **2008**, *78*, 113201.

[6] C. Deibel, A. Baumann, A. Wagenpfahl, V. Dyakonov, *Synth. Met.* **2009**, *159*, 2345.

[7] G. Sliaužys, G. Juška, K. Arlauskas, A. Pivirkas, R. Österbacka, M. Scharber, A. Mozer, N. S. Sariciftci, *Thin Solid Films* **2006**, *511-512*, 224.

[8] G. Juška, K. Genevičius, N. Nekrašas, G. Sliaužys, R. Österbacka, *Appl. Phys. Lett.* **2009**, *95*, 013303.

[9] C. Groves, N. C. Greenham, *Phys. Rev. B* **2008**, *78*, 155205.

[10] L. J. A. Koster, V. D. Mihailetchi, P. W. M. Blom, *Appl. Phys. Lett.* **2006**, *88*, 052104.

[11] L. J. A. Koster, V. D. Mihailetchi, H. Xie, P. W. M. Blom, *Appl. Phys. Lett.* **2005**, *87*, 203502.

[12] J. Gao, F. Hilde, H. Wang, *Synth. Met.* **1997**, *84*, 979.

[13] P. Schillinsky, C. Waldauf, C. J. Brabec, *Appl. Phys. Lett.* **2002**, *81*, 3885.

[14] J. K. J. van Duren, X. N. Yang, C. W. T. Bulle-Lieuwma, A. B. Sieval, J. C. Hummelen, R. A. J. Janssen, *Adv. Funct. Mater.* **2004**, *14*, 425.

[15] V. Dyakonov, *Thin Solid Films* **2004**, *451 – 452*, 493.

[16] I. Riedel, J. Parisi, V. Dyakonov, L. Lutsen, D. Vanderzande, C. J. Brabec, *Adv. Funct. Mater.* **2004**, *14*, 38.

[17] D. Gebeyehu, M. Pfeiffer, B. Maenning, J. Drechsel, A. Werner, K. Leo, *Thin Solid Films* **2004**, *451 – 452*, 29.

[18] M. Schubert, R. Steyrleuthner, S. Bange, A. Sellinger, D. Neher, *Phys. Status Solidi (a)* **2009**, *206*, 2743.

[19] B. Sun, G. Zou, X. Shen, X. Zhang, *Appl. Phys. Lett.* **2009**, *94*, 233504.

[20] W. U. Huynh, J. J. Dittmer, N. Teclemariam, D. J. Milliron, A. P. Alivisatos, *Phys. Rev. B* **2003**, *67*, 115326.

[21] J. J. Dittmer, *Ph.D. thesis*, University of Cambridge **2001**.

[22] A. M. Goodman, A. Rose, *J. Appl. Phys.* **1971**, *42*, 2823.

[23] L. J. A. Koster, E. C. P. Smits, V. D. Mihailetchi, P. W. M. Blom, *Phys. Rev. B* **2005**, *72*, 085205.

[24] V. D Mihailetchi, H. Xie, B. de Boer, L. J. A. Koster, P. W. M. Blom, *Adv. Funct. Mater.* **2006**, *16*, 699.